

Multi-shell gold nanowires under compression

This article has been downloaded from IOPscience. Please scroll down to see the full text article.

2001 J. Phys.: Condens. Matter 13 11531

(<http://iopscience.iop.org/0953-8984/13/50/312>)

View [the table of contents for this issue](#), or go to the [journal homepage](#) for more

Download details:

IP Address: 171.66.16.238

The article was downloaded on 17/05/2010 at 04:40

Please note that [terms and conditions apply](#).

Multi-shell gold nanowires under compression

G Bilalbegović

Department of Physics, University of Rijeka, Omladinska 14,51000 Rijeka, Croatia

Received 2 August 2001, in final form 20 September 2001

Published 30 November 2001

Online at stacks.iop.org/JPhysCM/13/11531

Abstract

Deformation properties of multi-wall gold nanowires under compressive loading are studied. Nanowires are simulated using a realistic many-body potential. Simulations start from cylindrical face-centred cubic (111) structures at $T = 0$ K. After annealing cycles, axial compression is applied to multi-shell nanowires for a number of radii and lengths at $T = 300$ K. Several types of deformation are found, such as large buckling distortions and progressive crushing. Compressed nanowires are found to recover their initial lengths and radii even after severe structural deformations. However, in contrast to the case for carbon nanotubes, irreversible local atomic rearrangements occur even under small compressions.

1. Introduction

Carbon nanotubes have been the focus of intensive research activity in the last few years [1]. Their electrical and thermal conductivities, as well as mechanical properties, are of great scientific and technological interest. Depending on the diameter and the helicity, carbon nanotubes can be either metallic or semiconducting, and exhibit quantum wire properties. Therefore, they are important for nanoelectronic devices. Some promising applications of carbon nanotubes are also based on their extraordinary mechanical properties. Investigations have shown that carbon nanotubes are among the strongest materials [1]. The effects of deformations and various defects are studied for single-wall and multi-wall tubes, as well as for ropes composed of carbon nanotubes [2–6]. It was found that very distorted carbon nanotubes return to their original form when loading is released. As a consequence, carbon nanotubes are useful in applications, for example as high-strength fibres, components of composite materials, and tips in scanning-probe microscopy [1–6].

The property of carbon nanotubes of deforming elastically is in part the outcome of the strength and rigidity of the graphitic bond. The cylindrical structure of the nanotubes increases their elasticity and strength. It is important to investigate the mechanical properties for cylindrical nanostructures made of other materials in which there is a different type of bonding. These investigations may shed light on the choice of optimal materials and structures for elements in nanomechanical devices. Metallic wires are important for applications. For

example, gold wires are already used as interconnections in chips. The miniaturization of electronic and mechanical devices requires investigations of very small wires whose diameters and lengths are in the range from 1 nm to 10 nm. Recently a technique for fabrication of metallic nanowires with diameters down to $d = 3$ nm was invented [7]. This method is based on the thickness resolution of molecular-beam epitaxy and formation of extremely precise templates for metal deposition. The mechanical properties of metallic nanowires until now have been investigated in experiments dealing with the contact between two pieces of metal. For example, metallic nanobridges were obtained in scanning tunnelling microscopy (STM) experiments [8], mechanically controllable break-junctions [9], and macroscopic table-top metallic contacts [10]. In this context the stability of tip-suspended nanowires, their behaviour under tensile strain, fracture properties, and conductance were investigated by means of molecular dynamics (MD) simulations and density functional theory calculations [11–24]. Mechanical properties of metallic nanocontacts under compressive strain are less well studied [13, 14, 18]. However, compression of free single-wall carbon nanotubes was investigated via MD simulations [3–6].

Multi-shell structures were obtained in MD simulations of finite and infinite gold nanowires [25–27]. Finite nanowires with radii around a nanometre and with a length/diameter ratio between 1 and 3 were studied [25, 26]. Cylindrical multi-shell structures were found for a length/diameter ratio between 2 and 3. Structures and melting of infinite gold nanowires with radii around a nanometre and an initial orientation along the (111), (110), and (100) directions were also investigated [27]. The results have shown that the formation of cylindrical shells is the most pronounced for an initial fcc (111) orientation. Similar gold nanostructures were found in experiments [28–30]. These studies were enabled by recent advances in microscopic techniques which now produce images of atomic scale resolution. Gold nanostructures were prepared by contacting a gold substrate with an STM tip, and they were simultaneously imaged using an ultrahigh-vacuum electron microscope [28, 30]. The conductance of these gold nanostructures was measured during retraction of the STM tip. It was found that the conductance is quantized in units of $2e^2/h$, where e is the electron charge and h is Planck's constant [28–30]. Stable and regular strands of gold atoms that are from one nanometre to several nanometres in length were observed. The diameters of these wires were around one nanometre. In MD simulations of Pb and Al ultrathin infinite wires at $T = 0$ K, several exotic structures were found, for example icosahedral and helical forms [31]. Similar simulation has been carried out for gold nanowires [24]. Aluminium and copper infinite nanowires were also simulated at room temperature and multi-shell and filled structures were obtained [32]. Recently Zach and co-workers developed a method for producing metallic wires with diameters ranging from 15 nanometres to 1.0 micrometers and lengths of up to half a millimetre [33]. They used the graphite substrate as a template for growing molybdenum wires. The mechanical strength of these nanowires was tested and it was found that they were sometimes able to bend at 90 degrees without breaking. In this work a MD simulation study of free multi-shell gold nanowires under axial compression at $T = 300$ K is presented. Our results show that these gold nanostructures are able to sustain very large values of strain and recover initial radii and lengths even after severe deformations. In the following, the interatomic potential, the wire preparation method, and the simulation details are described in section 2. Results and a discussion are presented in section 3. A summary and conclusions are given in section 4.

2. Computational method

The interaction between gold atoms was modelled by the well-tested embedded-atom potential [34]. It is known that embedded-atom potentials provide a satisfactory description of metallic bonding in the bulk, for surfaces, and for nanoparticles [35]. Unlike pair interactions, such as

the Lennard-Jones and Morse potentials, the embedded-atom model takes account of many-body effects in metals. The particular realization of the embedded-atom potential used here, the so-called glue model, has been shown to accurately reproduce experimental values for a wide range of physical properties of gold [34]. The classical MD simulation method was used. The equations of motion were integrated using a time step of $\Delta t = 7.14 \times 10^{-15}$ s. In all simulations presented in this work, the temperature control was realized through velocity rescaling of all active atoms.

It is known that bulk gold crystallizes in a face-centred cubic lattice. Initially, for nanowires at $T = 0$ K, atoms were arranged in a fcc structure with the (111) direction parallel to the axis of the wire. The prepared nanowires were approximately cylindrical in cross-section. All atoms whose radial distance from the nanowire axis was above a chosen value were removed. Several nanowires with length L_0 between 4 nm and 12 nm, number of atoms between 540 and 2067, and radius R_0 between 0.5 nm and 1.2 nm were investigated. All wires were first relaxed at $T = 0$ K. Then samples were heated to 1000 K. This was followed by a quench to $T = 0$ K, and heating to $T = 300$ K. In previous simulations, where structural and vibrational properties of finite gold nanowires were investigated, MD boxes in the annealing cycles were heated to 600 K [25,26]. However, it was found here that even finite nanowires are robust, and preserve their cylindrical structures when heated up to ~ 0.75 of the bulk melting temperature. Properties of nanowires under compression were investigated after evolution of 10^5 time steps at $T = 300$ K. As in previous simulations for finite [25,26] and infinite gold nanowires [27], after a preparation procedure, stable multi-shell cylindrical structures were obtained. In comparison with previous simulations of finite gold nanowires, a higher annealing temperature is applied here, and this produces more regular multi-shell structures. After equilibration, as in simulations of single-wall carbon nanotubes [3–6], the edge rings were fixed, and then compressive axial loading was applied. These simulations under compression were most often taken out to 2×10^4 time steps. It was checked that typical deformation patterns formed during this time did not change up to 10^5 time steps.

3. Results and discussion

Several structures of multi-shell wires at 300 K and before compression was applied are presented in figure 1. Figure 1(a) shows a three-shell structure with the central core. This type of multi-shell configuration with a single central strand of gold atoms forms most often. The nanowire with the smallest radius of those investigated forms a two-wall structure with a large empty core shown in figure 1(b). A core of two strands of atoms, as in the four-wall structure shown in figure 1(c), was also obtained.

Short and narrow nanowires (e.g., $R_0 = 0.9$ nm, $L_0 = 4$ nm) under compression exhibit only one morphological pattern. They progressively shorten when compression increases, but remain straight. As an exception, long and extremely narrow nanowires (e.g., $R_0 = 0.5$ nm, $L_0 = 12$ nm) under compression often crush into irregular ellipsoidal morphologies. Thicker short nanowires (e.g., $R_0 = 1.2$ nm, $L_0 = 8$ nm) show three morphological patterns. For small compressions these nanowires deform by rippling. However, rippling is less pronounced than in single-wall carbon nanotubes [6], and only isolated ripples appear. Under 16 GPa of stress, one end of the nanowire deforms more than the other. Such a deformation is shown in figure 2. For larger stress (≥ 32 GPa) these nanowires also deform by crushing, flatten, and preserve their cylindrical shapes. Nanowires return to the configuration with approximately the initial R_0 and L_0 when compression is released. The outer cylindrical surfaces of these straight wires are rougher than the initial ones.

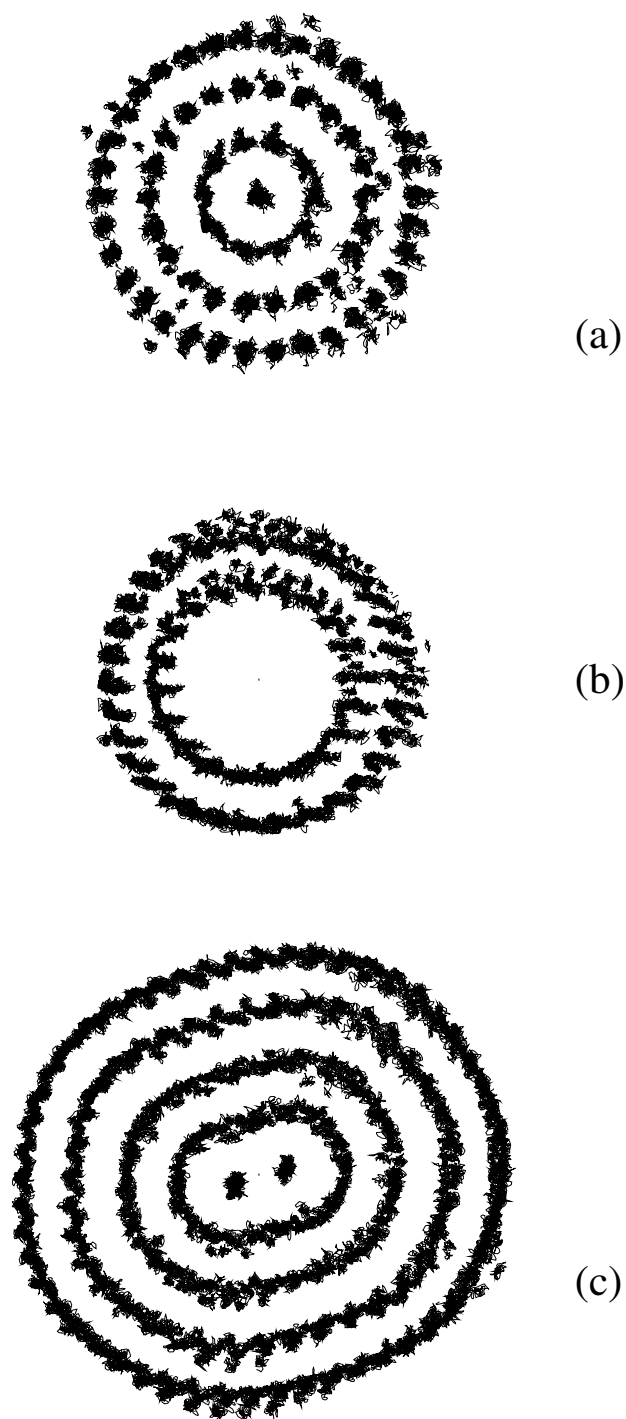


Figure 1. Top views of initially uncompressed multi-shell nanowires: (a) $R_0 = 0.9$ nm, $L_0 = 12$ nm; (b) $R_0 = 0.5$ nm, $L_0 = 12$ nm; (c) $R_0 = 1.2$ nm, $L_0 = 8.0$ nm. The trajectory plots refer to a time span of ~ 7 ps and include all atoms in a slice of thickness of 4 nm along the wire axis.

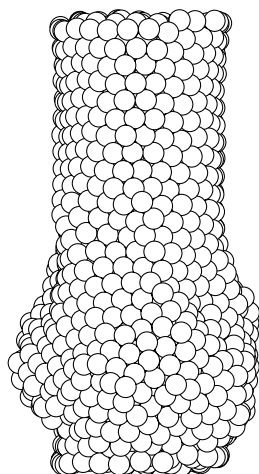


Figure 2. Deformation of a nanowire with $R_0 = 1.2$ nm and $L_0 = 8$ nm, under a stress of 19.23 GPa.

The most interesting behaviour is exhibited by long and narrow nanowires (e.g., $R_0 = 0.9$ nm, $L_0 = 12$ nm; shown in figure 3(a)). These slender nanowires under compression buckle and sometimes exhibit substantially distorted configurations. Figure 3(b) shows deformation of the nanowire shown in figure 3(a) under 4.81 GPa of stress. The structure formed in this sideways deformation is almost symmetric. Figure 4(a) shows a configuration of the

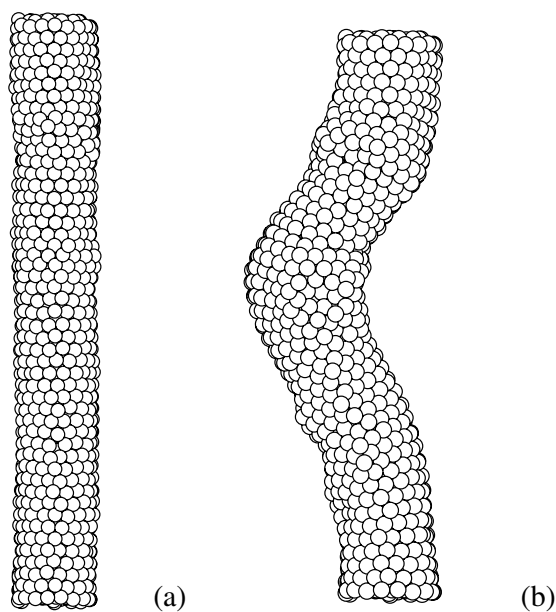


Figure 3. A nanowire with $R_0 = 0.9$ nm and $L_0 = 12$ nm: (a) the uncompressed configuration (a top view of the same nanowire is shown in figure 1(a)); (b) deformation of this nanowire under a stress of 4.81 GPa.

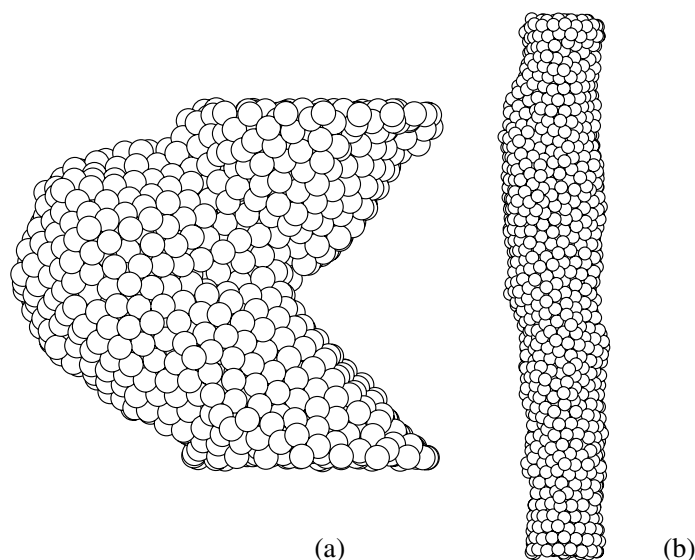


Figure 4. Structural changes in the nanowire shown in figure 3(a) and figure 1(a): (a) the nanowire deformed under a stress of 6.41 GPa; (b) the same nanowire simulated after the compression (producing the configuration shown in (a)) is released.

same nanowire under 6.41 GPa of stress. Although deformed substantially (figure 4(a)), this structure immediately straightens (figure 4(b)) when compression is released. This structural change takes place within just 7 ps of time evolution after loading is released. The resulting configuration (shown in figure 4(b) after 35 ps, i.e., 5×10^3 time steps) is less regular than the initial nanowire, but has the same average radius and length. In further simulations at the same temperature this nanowire does not change substantially up to 0.7 ns. The same stress of 6.41 GPa applied to the structure shown in figure 4(b) produces a buckled morphology similar to the one shown in figure 4(a). When loading is released in this repeated compression, the nanowire again returns to a straight form similar to the one shown in figure 4(b). Large buckling deformations (as shown in figures 3(b) and 4(a)) exist for average compressions. For the highest values of the stress, slender nanowires deform by crushing and flattening, and remain straight.

These simulations show that a multi-shell structure disappears under compression. The density plots in figure 5 illustrate the changes in a multi-shell structure under compression. For the stress of 3.2 GPa the shell structure is still present (figure 5(b)), whereas at 4.81 GPa the shells are much less pronounced (figure 5(c)). The shell structure is almost absent at 6.41 GPa (figure 5(d)). When compression is released, nanowires straighten, but their internal multi-shell structure only partially recovers in the simulation of 2×10^4 time steps. Disordering of a multi-shell structure is more pronounced in longer nanowires and for a higher applied stress. As in initial annealing cycles, it is possible to improve this partially ordered multi-shell structure by heating. In multi-shell gold nanowires, atomic rearrangements occur for the smallest applied stress. In contrast, carbon nanotubes up to certain values of stress are in the elastic regime. There, virtually no defects are found after compressive loading is released [3–6]. Beyond the elastic regime, carbon nanotubes deform plastically. In the plastic regime, as here for gold nanowires, compressed carbon nanotubes recover from severe structural deformations, but local atomic rearrangements exist.

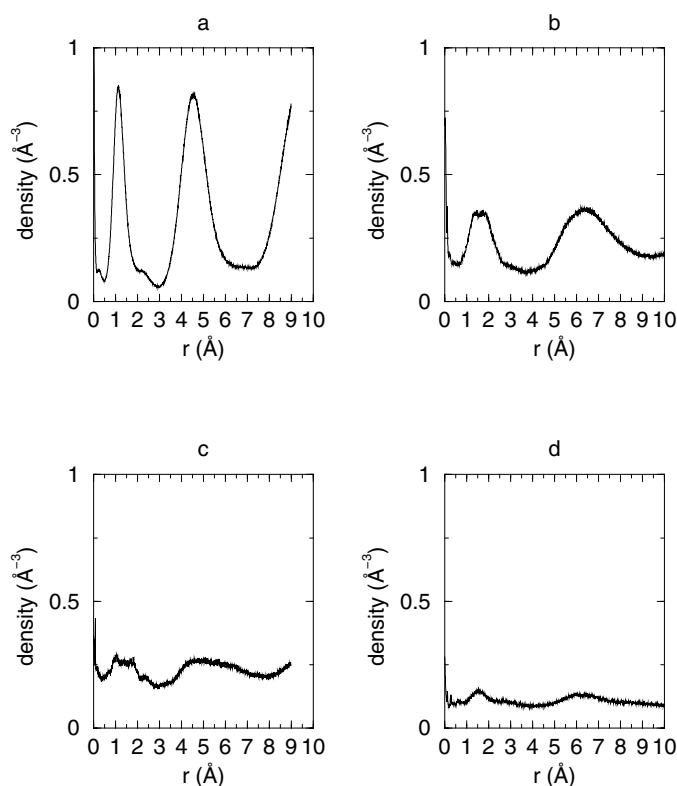


Figure 5. Radial density plots for a nanowire with $R_0 = 0.9$ nm, $L_0 = 12$ nm, under stresses of: (a) 0 GPa; (b) 3.2 GPa; (c) 4.81 GPa; (d) 6.41 GPa.

A plot of the stress versus the strain for several nanowires is presented in figure 6. All shells of multi-wall nanowires are stressed and it is assumed that the axial strain and stress are uniformly distributed over the cross-section. Therefore, in calculations of the stress the whole cross-sectional area of the nanowire is used. These results show that multi-shell gold nanowires are able to sustain a large compressive stress. Multi-shell gold nanowires at large compressions behave in a similar way to ropes of single-wall carbon nanotubes under pressure [36]. These ropes of nanotubes act as a mechanical energy store. This was attributed to the crushing and flattening of the tube cross-section. A flattening along the wire axis was found in this simulation for gold nanowires. These morphological patterns correspond to the vertical portions of the curves in figure 6. Therefore, because of the property of recovering their shapes even for large values of the strain, multi-shell gold nanowires also act as a mechanical energy store. Although the chemical bondings in carbon nanotubes and gold nanowires are different, the packing effects at nanometre length scales are also important. Regular axially symmetrical distributions of carbon nanotubes in ropes and cylindrical gold shells in nanowires enable them to store mechanical energy.

4. Conclusions

Molecular dynamics simulation was carried out to study deformations of multi-shell gold nanowires under axial compressive loading at $T = 300$ K. This simulation is based on a

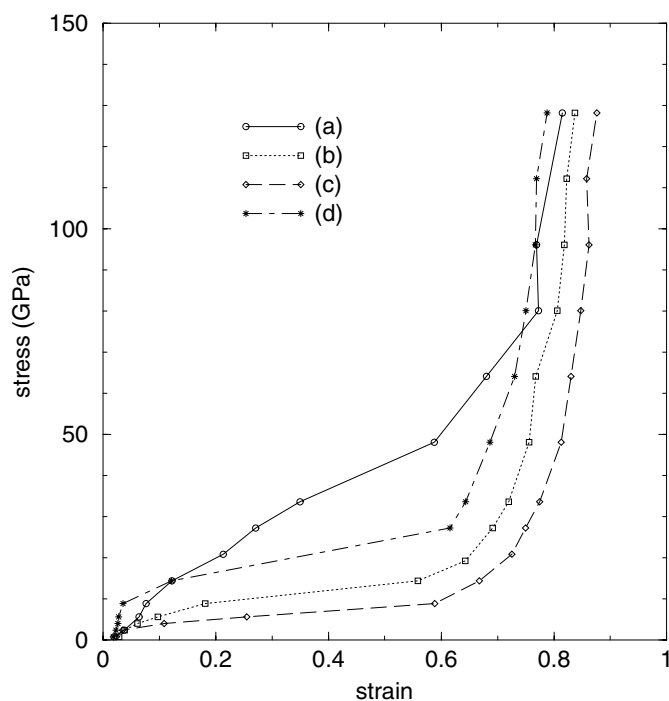


Figure 6. Stress versus strain curves: (a) $R_0 = 0.9$ nm, $L_0 = 4$ nm; (b) $R_0 = 0.9$ nm, $L_0 = 8$ nm; (c) $R_0 = 0.9$ nm, $L_0 = 12$ nm; (d) $R_0 = 1.2$ nm, $L_0 = 8$ nm.

well-tested embedded-atom potential. It was found that multi-shell nanowires are able to sustain large values of the compressive strain. The most interesting behaviour is shown by long and narrow nanowires where large buckling distortions without a failure are possible when axial compression is applied and then released. The property of carbon nanotubes of recovering without damage after large deformations was explained as a consequence of the carbon bonding in the graphite layer and the cylindrical structure of the tube. The simulation presented here shows that multi-shell gold nanowires, after large deformations, recover their cylindrical forms, as well as their initial radii and lengths. A similar result (i.e., that large bending deformations without breaking are possible) was recently obtained experimentally for molybdenum nanowires [33]. In contrast to carbon nanotubes, because of the different type of chemical bonding in gold, atomic rearrangements occur even under small compressions. As a result, defects and local structural changes are always present in gold nanowires when loading is released. The property of multi-shell gold nanowires of storing mechanical energy will be useful for applications. The mechanical properties of various metallic nanowires deserve further experimental and theoretical investigations.

Acknowledgments

This work was carried out under the HR-MZT project 119206 ‘Dynamical Properties of Surfaces and Nanostructures’ and the EC Research Action COST P3 ‘Simulation of Physical Phenomena in Technological Applications’.

References

- [1] McEuen P L 2000 *Phys. World* **13** 31
Schönenberger C and Forro L 2000 *Phys. World* **13** 37
Dai H 2000 *Phys. World* **13** 43
de Heer W A and Martell R 2000 *Phys. World* **13** 49
- [2] Yakobson B I and Avouris Ph 2001 *Carbon Nanotubes* ed M S Dresselhaus, G Dresselhaus and Ph Avouris (Berlin: Springer) p 287
- [3] Yakobson B I, Brabec C J and Bernholc J 1996 *Phys. Rev. Lett.* **76** 2511
- [4] Cornwell C F and Wille L T 1997 *Solid State Commun.* **101** 555
- [5] Srivastava D, Menon M and Cho K 1999 *Phys. Rev. Lett.* **83** 2973
- [6] Ozaki T, Iwasa Y and Mitani T 2000 *Phys. Rev. Lett.* **84** 1712
- [7] Natelson D, Willet R L, West K W and Pfeiffer L N 2000 *Appl. Phys. Lett.* **77** 1991
- [8] Pascual J I, Mendez J, Gomez-Herrero J, Baro A M, Garcia N and Binh V T 1993 *Phys. Rev. Lett.* **71** 1852
- [9] Muller C J, van Ruitenbeek J M and de Jongh L J 1992 *Physica C* **191** 485
- [10] Costa-Krämer J L, Garcia N, Garcia-Mochales P and Serena P A 1995 *Surf. Sci.* **342** L1144
- [11] Brandbyge M, Shjøtz J, Sørensen M R, Stoltze P, Jacobsen K W, Nørskov J K, Olsen L, Laegsgaard E, Stensgaard I and Besenbacher F 1995 *Phys. Rev. B* **52** 8499
- [12] Bratkovsky A M, Sutton A P and Todorov T N 1995 *Phys. Rev. B* **52** 5036
- [13] Torres J A and Saenz J J 1996 *Phys. Rev. Lett.* **77** 2245
- [14] Landman U, Luedtke W D, Salisbury B E and Whetten R L 1996 *Phys. Rev. Lett.* **77** 1362
- [15] Barnett R N and Landman U 1997 *Nature* **387** 788
- [16] Mehrez H and Ciraci S 1997 *Phys. Rev. B* **56** 12 632
- [17] Finbow G M, Lynden-Bell R M and McDonald I R 1997 *Mol. Phys.* **92** 705
- [18] Häkkinen H and Manninen M 1998 *Europhys. Lett.* **44** 80
- [19] Taraschi G, Mozos J L, Wang C C, Guo H and Wang J 1998 *Phys. Rev. B* **58** 13 138
- [20] Nakamura A, Brandbyge M, Hansen L B and Jacobsen K W 1999 *Phys. Rev. Lett.* **82** 1538
- [21] Ikeda H, Qi Y, Cagin T, Samwer K, Johnson W L and Goddard W A 1999 *Phys. Rev. Lett.* **82** 2900
- [22] Branicio P S and Rino J P 2000 *Phys. Rev. B* **62** 16 950
- [23] Tosatti E, Prestipino S, Kostlmeier S, DalCorso A and Di Tolla F D 2001 *Science* **291** 288
- [24] Wang B, Yin S, Wang G, Buldum A and Zhao J 2001 *Phys. Rev. Lett.* **86** 2046
- [25] Bilalbegović G 1998 *Phys. Rev. B* **58** 15 412
- [26] Bilalbegović G 2000 *Mol. Simul.* **24** 87
- [27] Bilalbegović G 2000 *Solid State Commun.* **115** 73
- [28] Ohnishi H, Kondo Y and Takayanagi K 1998 *Nature* **395** 781
Kondo Y and Takayanagi K 2000 *Science* **289** 606
- [29] Yanson A I, Rubio Bollinger G, van den Brom H E, Agrait N and van Ruitenbeek J M 1998 *Nature* **395** 783
- [30] Rodrigues V, Fuhrer T and Ugarte D 2000 *Phys. Rev. Lett.* **85** 4124
- [31] Gulseren O, Ercolessi F and Tosatti E 1998 *Phys. Rev. Lett.* **80** 3775
- [32] Bilalbegović G 2000 *Comput. Mater. Sci.* **18** 333
- [33] Zach M, Ng K and Penner R 2000 *Science* **290** 2120
- [34] Ercolessi F, Parrinello M and Tosatti E 1988 *Phil. Mag. A* **58** 213
- [35] Daw M S, Foiles S M and Baskes M I 1993 *Mater. Sci. Rep.* **9** 251
- [36] Chesnokov S A, Nalimova V A, Rinzler A G, Smalley R E and Fisher J E 1999 *Phys. Rev. Lett.* **82** 343